Indonesian Journal on Geoscience Vol. 13 No. 3 December 2026: 409-422

INDONESIAN JOURNAL ON GEOSCIENCE
Geological Agency
Ministry of Energy and Mineral Resources

Journal homepage: https://ijog.geologi.esdm.go.id
ISSN 2355-9314, e-ISSN 2355-9306

Extreme Drought Characteristics in Java (1960-1965)

Muhshonati Syahidah[1], Rusmawan Suwarman[2], and Dhara Brawijaya[3]

[1]Doctoral Program of Earth Science, Faculty of Earth Science and Technology, Bandung Institute of Technology, Indonesia
[2]Department of Earth Science, Faculty of Earth Science and Technology, Bandung Institute of Technology, Indonesia
[3]Master Program of Environmental Engineering, Faculty of Civil and Environmental Engineering, Bandung Institute of Technology, Indonesia

Corresponding author: muhshonatisyahidah@gmail.com
Manuscript received: January 13, 2025; revised: July 21, 2025;
approved: May 19, 2026; available online: August 12, 2026

Abstract - This study examines the characteristics of the extreme drought experienced in Java between 1960 and 1965, a period marked by consecutive years of dry conditions. The research employs the Standardized Precipitation Index (SPI) to quantify meteorological drought and to assess extreme events as defined by the World Meteorological Organization (WMO), focusing on magnitude, duration, and spatial extent. The analysis identifies extreme drought episodes in 1960 and 1965, with 1964 exhibiting the most extreme magnitude, indicated by SPI-12 values of ≤ -2. These droughts were notably prolonged, with a duration of up to thirty-nine months (from December 1960 to October 1964), and spatial analysis reveals that the southern half of Java was most affected, covering nearly half the region. Further analysis explores the influence of major climate anomalies, including El Niño (Niño 3.4), the Indian Ocean Dipole (IOD), the Pacific Decadal Oscillation (PDO), and other climate indices. Spatial correlation analysis confirms that ENSO and IOD were the dominant drivers, with Niño 3.4 and DMI showing strong negative correlations with SPI-12, particularly across Central and East Java. In contrast, the PDO exhibited a positive correlation with SPI-12, suggesting it may have played a moderating role by enhancing rainfall during its positive phase. The study concludes that drought duration is a critical dimension in defining extreme drought in Java and that accounting for both interannual (ENSO, IOD) and decadal (PDO) variability is essential for improving drought risk forecasting and resilience strategies in vulnerable regions.

Keywords: drought, magnitude, duration, spatial extent, Standardized Precipitation Index, Niño 3.4, IOD, PDO

How to cite this article:
Syahidah, M., Suwarman, R., and Brawijaya, D., 2026. Extreme Drought Characteristics in Java (1960-1965). *Indonesian Journal on Geoscience*, 13 (3), p.409-422. DOI: 10.17014/ijog.13.3.409-422

Introduction

Background

Drought on a global scale has become a pressing concern, with increasing frequency, duration, and intensity reported worldwide. Studies have highlighted significant drought trends in North America, Europe, Asia, and Africa, driven by climatic variability and anthropogenic influences (Dai, 2011; Spinoni *et al*., 2017). Extreme weather and climate events have become more frequent and intense, leading to more natural disasters like floods and severe droughts (Cunha *et al*., 2019) . The increase in drought frequency, duration, and severity is found to be significant in Africa, eastern Asia, the Mediterranean region, and southern Australia (Spinoni *et al*., 2017). Similarly, Java faces a high risk of drought across most provinces (Avia *et al*., 2023). Drought is a complex natural hazard with significant destructive impacts on agriculture, the ecological environment, and socioeconomic systems, especially extreme drought (Guo *et al*., 2020) . Focusing on meteorological drought, it arises when seasonal or annual rainfall falls below its long-term average. The consequences of meteorological drought include diminished water supply, crop failures, reduced agricultural productivity, habitat disruption, and negative impacts on economic and social activities (Mishra and Singh, 2010; Riebsame *et al*., 2019). Prolonged droughts can worsen water scarcity, disrupt hydropower-dependent energy production (Tallaksen and Lanen, 2004), and harm riverine ecosystems, leading to a loss of aquatic biodiversity (Loon *et al*., 2014).

Extreme drought conditions in Java show a strong link with variability from the El Niño-Southern Oscillation (ENSO). D'Arrigo *et al*. (2006) demonstrated a robust historical connection between ENSO variability and drought intensity in Java, using tree-ring records to reconstruct monsoon drought signals. Studies indicate that this period coincided with both regional and global climatic anomalies, as El Niño events typically reduce rainfall across the Indonesian Archipelago (Lee, 2015; Ropelewski and Halpert, 1987). Suwarman *et al*. (2017) further demonstrated that during El Niño years, deep convective activity over the Maritime Continent is significantly suppressed, resulting in reduced rainout and decreased overall precipitation across the region. Reduced rainfall during consecutive El Niño years has been associated with severe drought and substantial agricultural losses in Southeast Asia (Tangang *et al*., 2007). Additionally, the Indian Ocean Dipole (IOD), particularly when in a positive phase, has been shown to intensify drought conditions by further suppressing rainfall in the region (Phan-Van *et al*., 2022; Saji *et al*., 1999).

In addition to ENSO and IOD, the Pacific Decadal Oscillation (PDO) may also modulate drought variability, because it represents a long-lived El Niño-like pattern of sea surface temperature variability in the Pacific Ocean, with warm or positive phases and cool or negative phases that can influence large-scale climate anomalies (Ul Hassan and Ahmad Nayak, 2021). PDO can also modulate the impacts of ENSO and IOD on Indonesian monsoon rainfall variability, particularly during the dry season, thereby contributing to drought conditions in several regions of Indonesia (Mulsandi *et al*., 2023).

These interactions raise important considerations regarding the severity of droughts in terms of magnitude, duration, and spatial extent. Rohmat *et al*. (2023) used the SPI index to show how global atmospheric circulations, including ENSO and IOD, drive water deficits across Indonesian watersheds. Understanding these extreme events is crucial, not only for historical climate diagnostics but also for developing adaptive frameworks for drought preparedness and early warning (Irawan and Komori, 2025).

This study aims to identify the characteristics of extreme drought events based on their magnitude, duration, and spatial extent on Java Island from 1960 to 1965 and to analyze the major climatic phenomena that coincided with these episodes. The focus is on meteorological droughts, analyzed using the Standardized Precipitation Index (SPI). One of the key advantages of SPI is its ability to normalize precipitation deficits across multiple timescales, enabling spatial and temporal comparison of drought severity (McKee *et al*., 1993). Drought classifications in this study follow the World Meteorological Organization (WMO) definition of extreme events as those reaching SPI values of -2.0 or lower (WMO, 2012). This historical perspective highlights how prolonged dry periods can lead to critical impacts. Ultimately, the value of this research lies in offering more profound insights into past extreme climatic conditions and supporting proactive, data-informed policies to mitigate future drought risks (Irawan and Komori, 2025; Rohmat *et al*., 2023).

Materials and Methods

Material

The research focuses on identifying meteorological extreme drought events in Java from 1960 to 1965. According to the WMO, extreme drought identification requires the analysis of three key parameters: magnitude (severity), duration, and spatial extent. (WMO, 2023). The index used to describe it is SPI, which was calculated at time scales of 6, 12, and 24 months. In accordance with McKee *et al*. (1993), extreme drought events were defined as periods when values of SPI ≤ -2.

The primary or baseline dataset used is the Global Precipitation Climatology Centre (GPCC) dataset, which provides monthly precipitation data at a spatial resolution of 0.25°×0.25°. The data used in this study cover the period from 1891 to 2020. In addition to examining potential teleconnections with drought occurrence in Java, large-scale climate variability was considered. The dataset indices that were used are Niño 3.4, the Pacific Decadal Oscillation (PDO), the Northern Oscillation Index (NOI), the Atlantic Multidecadal Oscillation (AMO), and the Atlantic Meridional Mode (AMM) (Smith *et al*., 2015) obtained from the NOAA site (https://psl.noaa.gov/data/timeseries/month/).

Methods

Methods to investigate and to characterize extreme drought events in Java from 1960 to 1965 can be carried out through the following steps. First, the SPI is calculated at 6-, 12-, and 24-month time scales based on precipitation data from GPCC. SPI was first computed for each grid cell across Java using the gamma probability distribution fitted to precipitation data and then standardized to the normal distribution (Equation 1). Subsequently, spatial averaging was performed to derive domain-level drought indicators. This procedure allowed for the assessment of both localized and region-wide drought characteristics. Then, extreme droughts were defined as periods when SPI values fall below -2, as defined by McKee *et al*. (1993) as follows:

$$g(x) = \frac{1}{\beta\alpha\Gamma(\alpha)} x^{\alpha-1} e^{\frac{-x}{\beta}} \quad \text{..........................(1)}$$

where:

$g(x)$ is the probability density function (PDF) of the gamma distribution,

$\alpha > 0$ is the shape parameter and $\beta > 0$ is the scale parameter,

$x > 0$ is the total monthly rainfall, and $\Gamma(\alpha)$ is the gamma function.

The next step the drought events are further characterized by their magnitude, duration, and intensity. Magnitude refers to the intensity of an event, measured by how far it deviates from a defined baseline or threshold. Duration describes the length of time the event persists, starting from when the threshold is first exceeded until conditions return to normal. Spatial extent represents the geographic area affected by the event, often expressed as the proportion of locations. Due to limited precipitation data availability in Indonesia during the 1960s, the spatial extent was evaluated indirectly using gridded SPI outputs derived from GPCC data. The total area of grid cells with SPI ≤ -2 was calculated and expressed as a percentage of the total land area of Java Island, representing the proportion of land affected by extreme drought during each event.

To explore the relationship between drought events and climate anomalies, this study analyzes several climate indices, including Niño 3.4, the Pacific Decadal Oscillation (PDO), the Northern Oscillation Index (NOI), The Atlantic Multidecadal Oscillation (AMO), and The Atlantic Meridional Mode (AMM). Correlation analyses and Principal Component Analysis (PCA) (Equation 2) were applied to identify the most influential climate drivers during the study period. The SPI results from the previous calculation are subjected to PCA to extract the dominant temporal patterns. The first principal component (PC1) explains the dominant variance in the dataset. PC1 is a linear combination of the observed variables x_j, where j= 1, 2, …, p, representing the number of variables:

$$PC1 = w_{(1,1)}x_{(1)} + w_{(1,2)}x_{(2)} + \cdots + w_{(1,p)}x_{(p)} \quad ...(2)$$

The PC-1, which accounts for the largest contribution to SPI variability was then examined using Pearson correlation with the climate indices (Equation 3). This comprehensive methodological framework provides a robust evaluation of extreme drought events and their connections to large-scale climatic factors, as illustrated in Figure 1.

$$r = \frac{\sum(x_i - \bar{x})(y_i - \bar{y})}{\sqrt{\sum(x_i - \bar{x})^2 (y_i - \bar{y})^2}} \quad ....(3)$$

where:
r is correlation coefficient,
x_i is values of the x-variable in a sample,
$\bar{x}$ is mean of the values of the x-variable,
y_i is values of the y-variable in a sample,
$\bar{y}$ and is mean of the values of the y-variable.

Result and Analysis

To evaluate drought severity, the Standardized Precipitation Index (SPI) was computed at multiple timescales: SPI-6, SPI-12, and SPI-24. The SPI-6 primarily reflects seasonal drought trends, whereas the SPI-12 captures more pronounced drought extremes, indicating sustained dry periods over the annual scale. In contrast, the SPI-24 may not exhibit distinct extremes due to the smoothing effect of intermittent wet months within the aggregated data. Figure 2 illustrates the SPI across these various timescales. The SPI-12 for Java Island from 1900 to 2020 reveals a sequence of successive droughts between 1960 and 1964. Each panel includes a black box highlighting the 1960–1965 period to facilitate comparison among SPI-6, SPI-12, and SPI-24. This finding aligns with the Palmer Drought Severity Index reconstruction by D'Arrigo et al. (2006), which also indicated that Java Island experienced consecutive extreme drought conditions from 1960 to 1965 (see their Figure 2).

One of the signs of extreme events, as noted by the WMO, is magnitude. McKee *et al.* (1993) establishes a threshold of -2 for defining extreme drought magnitude. Based on the SPI-12 values depicted in Figure 3, the extreme drought threshold was only reached once between 1960 and 1965, specifically in 1964. Thus, in terms

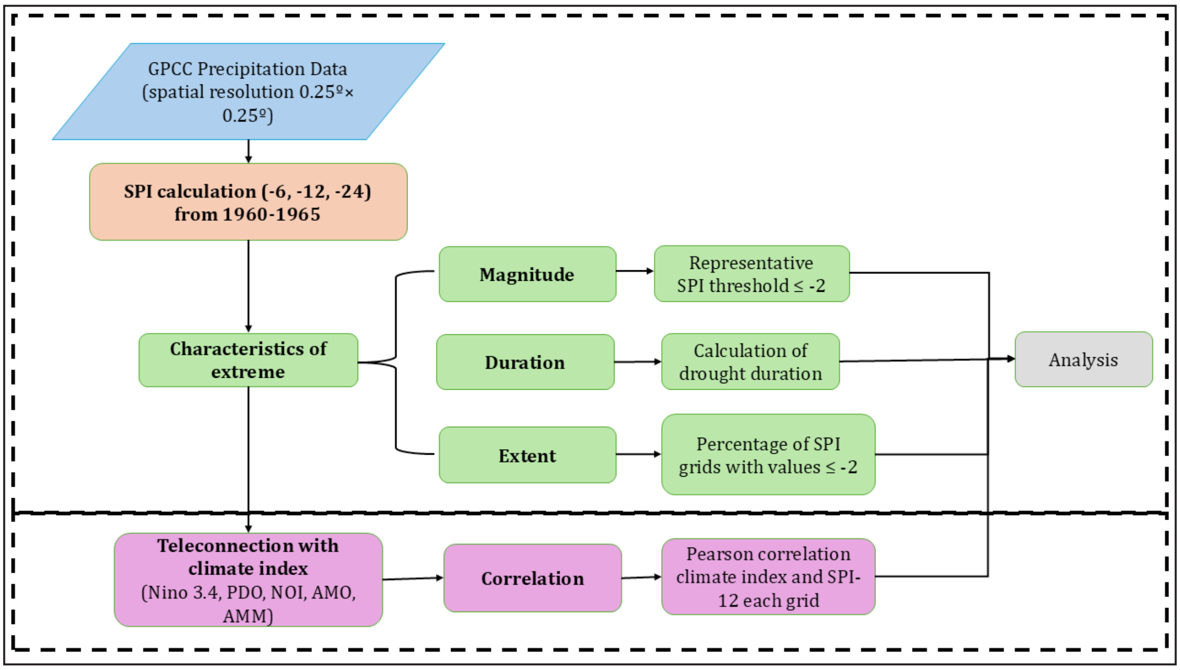

Figure 1. Methodological framework for characterizing extreme drought in Java, and for analyzing its climate teleconnections (1960-1965).

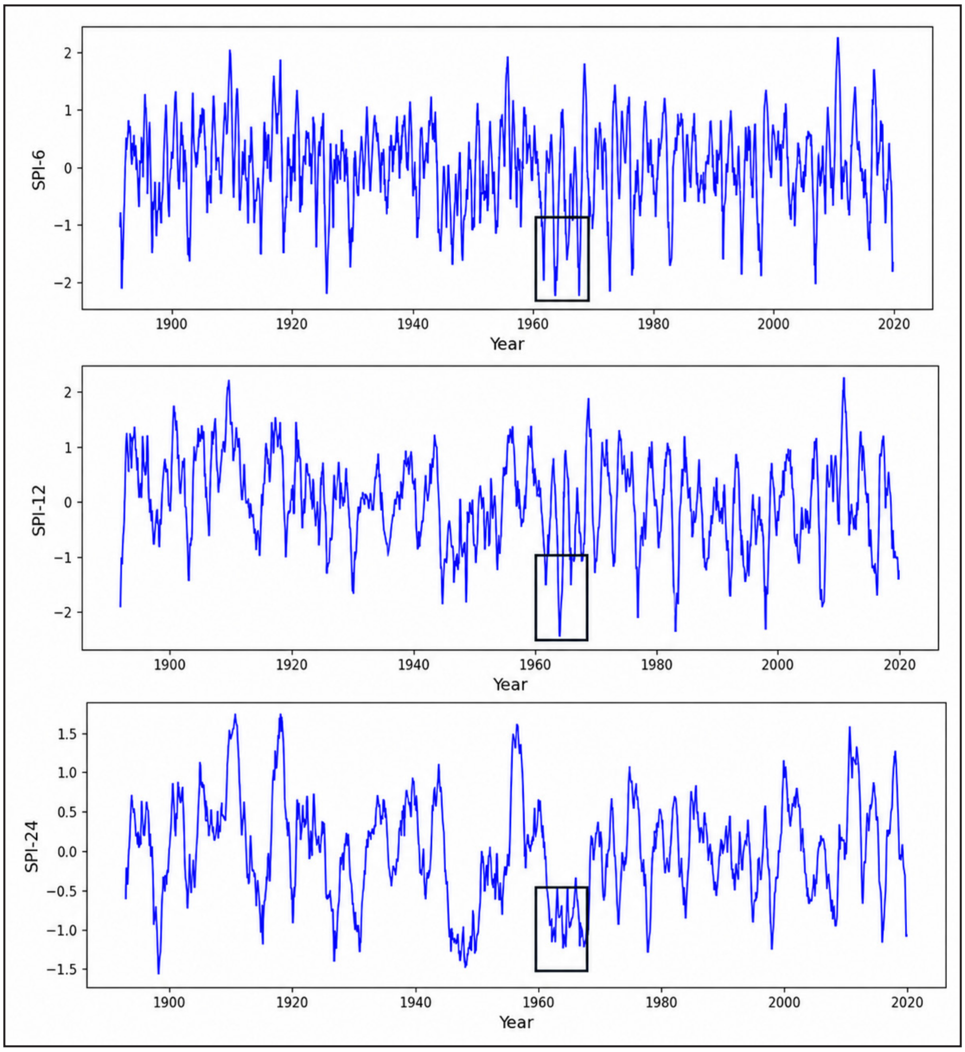

Figure 2. Time series of SPI for Java Island from 1900 to 2020; (a). SPI 6-Month; (b). SPI 12-month; (c). SPI 24-month.

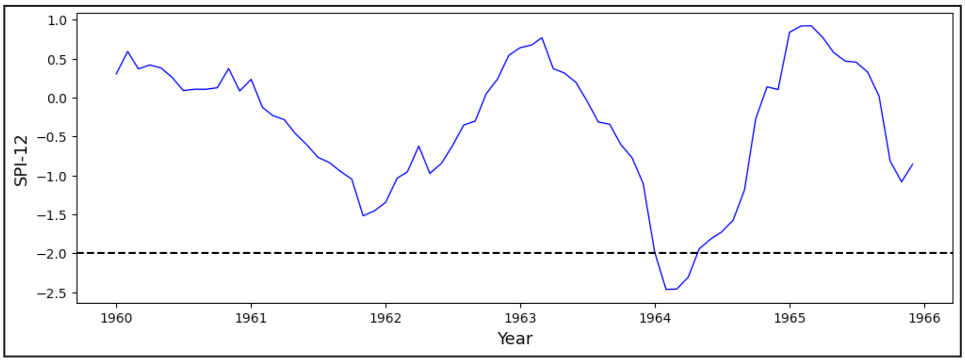

Figure 3. SPI 12-month scales for Java 1960-1965.

of magnitude, only the year 1964 qualifies as an extreme drought event, while the other years did not reach the threshold for extreme classification.

Drought duration refers to the time between the onset and end of a drought event. According to the McKee classification, an extreme drought occurs when the value of monthly SPI is less than or equal to -2.0 for a specific period. Extreme drought ends when the monthly value of SPI is above or equal to zero. Figure 4 and Figure 5 illustrate the duration

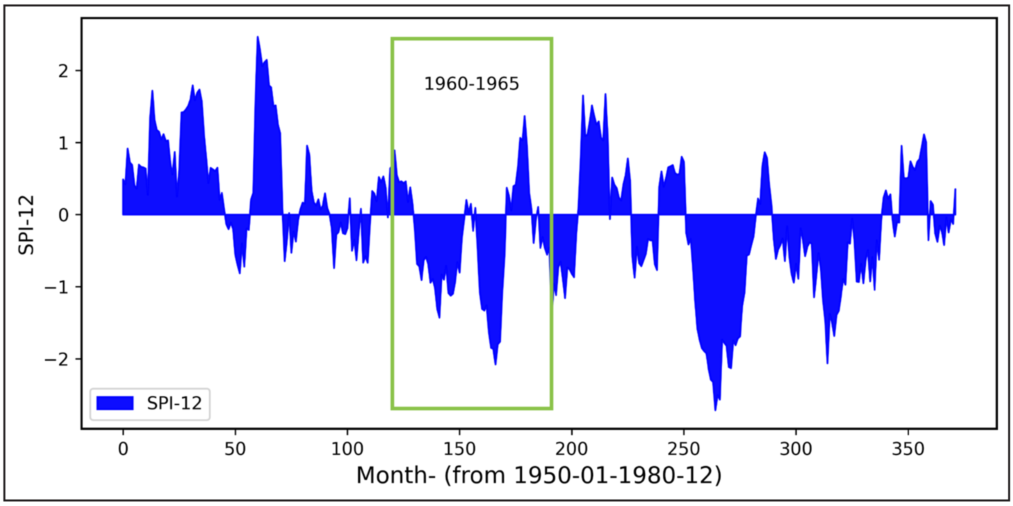

Figure 4. The events of drought during 1950-1980 in Java Island. The green box highlights the drought duration that occurred from 1960 to 1965.

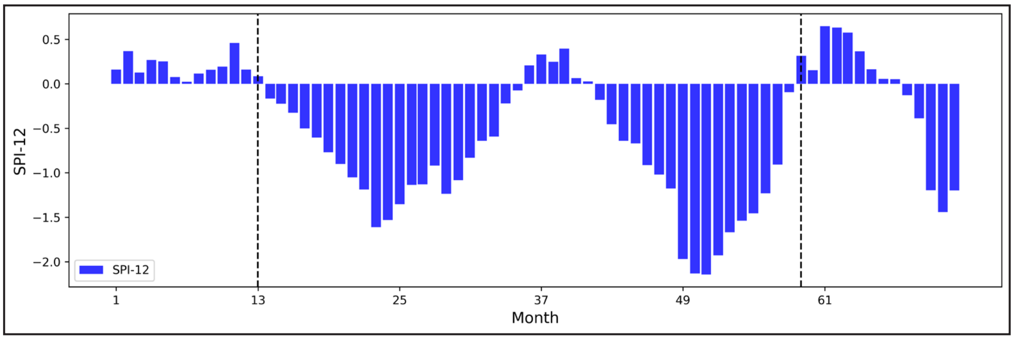

Figure 5. The same with Figure 4 but for 1960-1965 .

of extreme drought in Java . According to Figure 4, the period from 1960 to 1965 was marked by the green box. The time series reveals frequent dry conditions (SPI < 0) with varying intensity, including several pronounced extreme drought events where SPI values drop below -2. Some of these events persist over extended periods, indicating that drought severity was driven not only by magnitude but also by duration.

Figure 5, with vertical dashed lines, indicates the onset and end of an extreme drought event, and the duration is derived from the SPI-12 timescale. The event started in December 1960 and ended in October 1964, yielding a total duration of thirty-nine months .

The prolonged drought episode from 1960 to 1965, with a pronounced peak in 1964 as highlighted by the red dashed line, is clearly illustrated in Figure 6 . The figure shows the average drought duration over Java for 1891–2019 based on GPCC precipitation data. SPI-12 was computed for each grid cell, followed by drought duration estimation and spatial averaging across the island. Blue bars indicate normal to moderate drought conditions (SPI < 0), while red bars represent extreme drought events (SPI ≤ -2), following McKee *et al.* (1993).

Notably, the period 1960-1965 exhibits a pronounced extreme drought signal, characterized by SPI values below -2 and relatively long durations, indicating a persistent and high-magnitude drought event over the region. The time series of average drought duration (1891-2020) shows a distinct peak around 1964, far exceeding values observed in other years. This highlights the 1960-1965 period as the most persistent and severe drought event within the entire observational record.

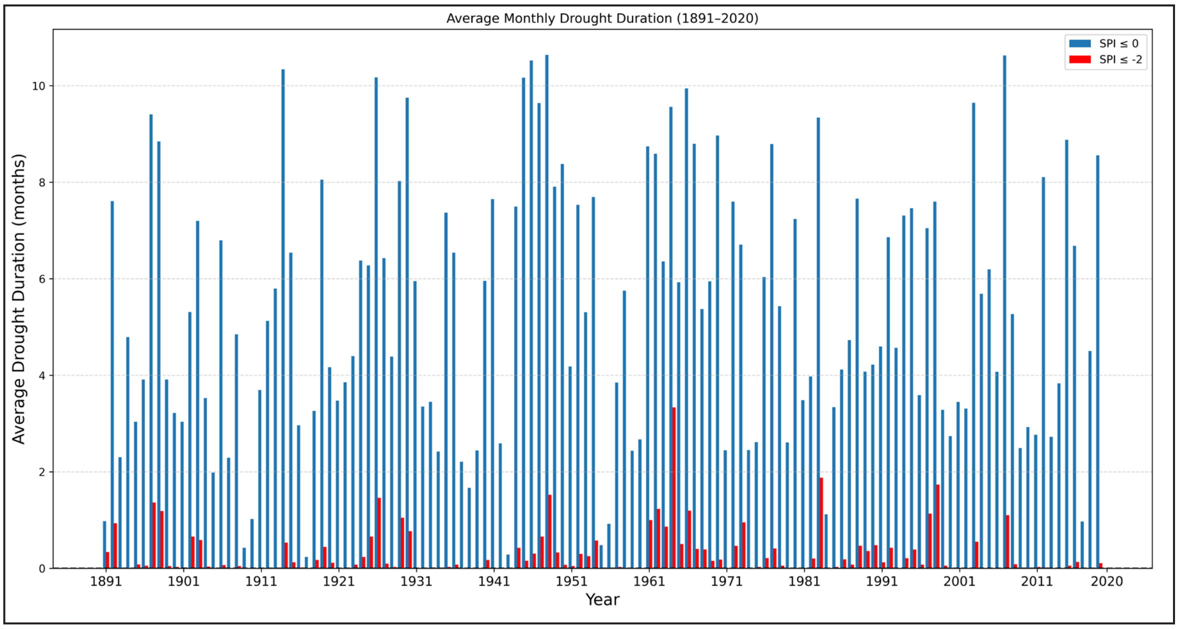

Figure 6. The yearly average duration (in months) of drought events from 1891 to 2020 .

While the preceding section addresses the temporal variability of drought duration, the subsequent analysis investigates its spatial extent, defined by geographical coverage. The spatial distribution of SPI-12 from 1960 to 1965 (Figure 7) reveals considerable fluctuations in both the extent and intensity of drought across Java during this period. Each panel in Figure 7 represents the month with the lowest SPI-12 values for each year, corresponding to extreme drought conditions. This selection highlights periods when drought reaches its most critical intensity. Dark brown represents extreme drought, while E indicates the area affected by it.

In 1960, drought conditions were almost nonexistent (E = 0.00%), but the affected area gradually increased in the following years, reaching its peak in 1964 with an extent of 58.27%. This indicates a progressive drying trend throughout the early 1960s. Figure 7 also shows that severe

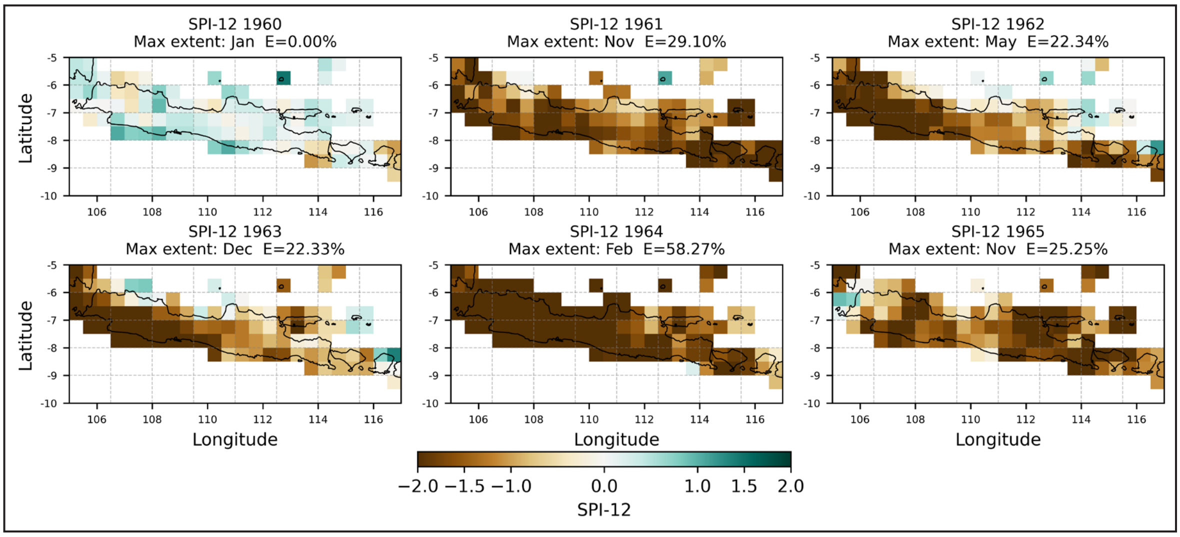

Figure 7. Drought extent 1960-1965 in Java Island (Extreme drought is represented by dark brown; E represent that area of extreme drought).

droughts, represented by darker brown shades (SPI-12 < -1.5), were predominantly concentrated in central and eastern Java. Furthermore, the timing of maximum drought extent varied between years, from January in 1960, November in 1961 and 1965, May in 1962, and December in 1963 to February in 1964, suggesting that the peak of dryness did not occur in the same season each year. Overall, the results suggest a shift toward drier climatic conditions, potentially influenced by large-scale climate variability. To further understand these fluctuations, several climate indices will be examined, including Niño 3.4, The Pacific Decadal Oscillation (PDO), The Indian Ocean Dipole (IOD), The Northern Oscillation Index (NOI), The Atlantic Multidecadal Oscillation (AMO), and The Atlantic Meridional Mode (AMM), all of which may play important roles in modulating rainfall variability and drought occurrence across Indonesia.

The Niño 3.4 index is used to define El Niño and La Niña events, with the threshold values classified by BMKG as follows: moderate (1.0-2.0) and strong (≥≥2.0). The PDO reflects long-term variations in North Pacific Sea surface temperatures and can modulate the influence of ENSO. When ENSO occurs during a positive PDO phase, the associated drought signal can be amplified. This phenomenon has been observed globally and may apply to the Indonesian region where rainfall deficits become more pronounced under the combined forcing (Wang *et al*., 2014). These climatic indices not only influence individual events but also interact across multiple time scales, shaping the overall drought variability in the region.

Figure 8 presents the standardized time series of SPI-12 alongside multiple climate indices from 1950 to 1970, highlighting distinct temporal patterns and interactions. The SPI-12 curve reveals pronounced drought events around 1957-1958 and 1964-1965, both of which align with peaks in the Niño 3.4 index, indicating strong El Niño activity. Short-term indices such as Niño 3.4, SOI, and IOD exhibit sharp interannual variability, closely tracking with drought-wet cycles in SPI-12. For example, the simultaneous rise of Niño 3.4 and positive IOD during 1964-1965 corresponds with deep SPI-12 troughs, supporting the role of ENSO-IOD coupling in intensifying drought conditions.

In contrast, decadal indices like PDO, AMO, and AMM display slower, more gradual fluctuations. These longer-term signals do not directly coincide with drought extremes but may provide a broader climatic backdrop that influences drought persistence. The shaded period (1960-1965) highlights a complex phase where short- and long-term indices overlap, suggesting that extreme droughts in Java are shaped by both immediate

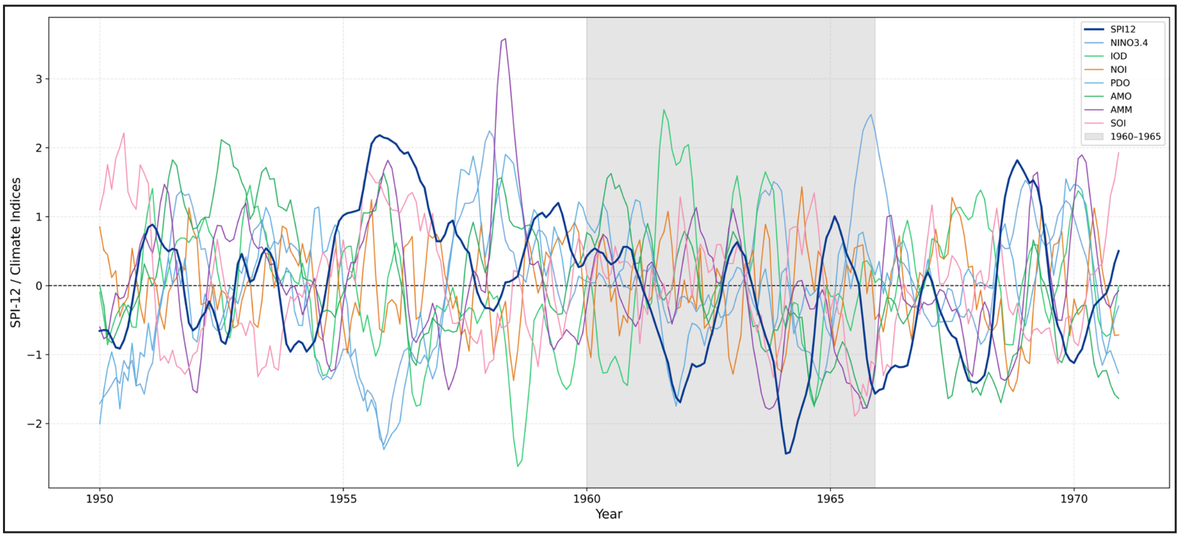

Figure 8. Climate indices with SPI-12 in Java Island 1950-2000.

ENSO-IOD forcing and underlying decadal variability. This reinforces the need to integrate both interannual and low-frequency climate drivers in frameworks for assessing drought risk.

Figure 9 focuses on the interannual variability of SPI-12 and selected climate indices, specifically Niño 3.4, IOD, and NOI, during the 1950-1970 period. The SPI-12 series (dark blue) shows marked drought phases around 1961-1962 and 1964-1965, which correspond with positive peaks in the Niño 3.4 index, confirming the strong influence of El Niño in suppressing rainfall and inducing droughts in Java. Conversely, La Niña periods (negative Niño 3.4 values) generally align with wetter conditions, as indicated by rising SPI-12 values, further reinforcing the expected ENSO-rainfall relationship.

The IOD (orange line) occasionally mirrors Niño 3.4, particularly during 1961–1962 and 1964-1965, where positive IOD phases coincide with El Niño, intensifying drought conditions. This alignment highlights the amplifying effect of ENSO-IOD coupling on hydrological deficits. In contrast, the NOI (green) shows relatively weak and inconsistent patterns throughout the period, indicating limited or nonsystematic correlation with SPI-12 at the interannual scale. Overall, the figure reinforces that ENSO and IOD are the dominant interannual drivers of extreme drought variability in Java, especially when their positive phases overlap.

Figure 10 shows the relationship between SPI-12 and key decadal climate indices, PDO, AMO, and AMM, during the 1950-1970 period. The SPI-12 curve (dark blue) continues to show prominent inter-annual drought-wet variability, with a pronounced drought around 1964-1965. Interestingly, this drought phase coincides with a positive phase of the PDO, not a negative one as previously stated, suggesting that in this specific case, the PDO may not be inversely related to drought severity in Java during the 1960s.

Meanwhile, The AMO (orange) and AMM (green) display slow, low-amplitude oscillations with no consistent alignment to SPI-12 extremes. Their patterns appear decoupled from the sharp fluctuations in SPI-12, indicating a limited or indirect role in modulating short-term droughts over Java. Overall, the figure suggests that decadal indices such as PDO, AMO, and AMM may provide a broader climatic background but do not act as primary drivers of inter-annual drought variability during the 1960-1965 period.

The three figures collectively illustrate a layered climate hierarchy influencing rainfall variability in Indonesia. Short-term SPI-12 fluctuations are closely linked to ENSO and IOD dynamics, which consistently produce immediate drought-wet responses at the inter-annual scale. This is especially evident during strong El Niño and positive IOD phases, which coincide with significant SPI-12 drops over Java. In contrast,

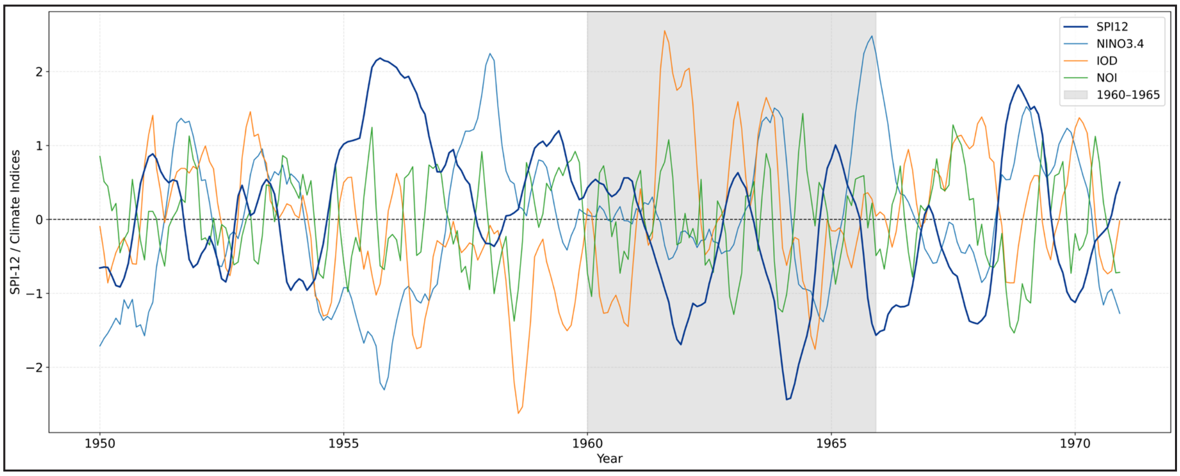

Figure 9. Climate indices inter-annual variability with SPI-12 in Java Island in 1950-1970.

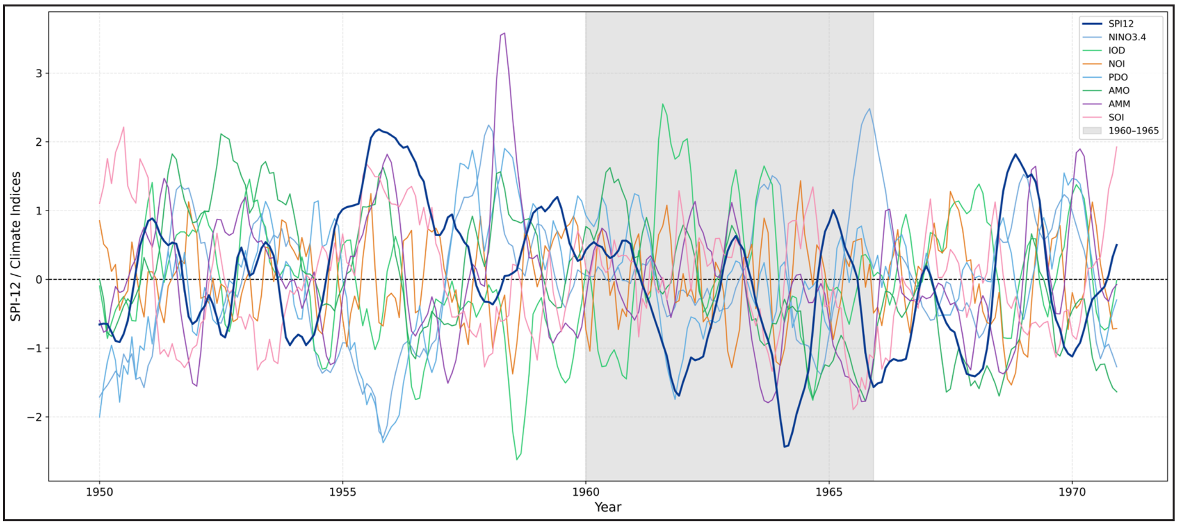

Figure 10. Climate indices' decadal to multidecadal variability with SPI-12 in Java Island in 1950-2000.

decadal indices such as PDO, AMO, and AMM show slower, more gradual variability with no consistent relationship to drought extremes, suggesting their role may be indirect or background-modulating rather than causal.

Together, the combined temporal and spatial analyses highlight how inter-annual climate drivers, especially ENSO-IOD coupling, dominate drought variability. Decadal oscillations may contribute to longer-term context but do not exert direct control over drought onset or severity. The correlation patterns across the figures further quantify these relationships, reinforcing that Niño 3.4 and IOD are the most influential indices during the 1960-1965 drought events in Java.

The correlation conducted between SPI-12 (as illustrated in Figure 11) and the four indices revealed significant relationships. Specifically,

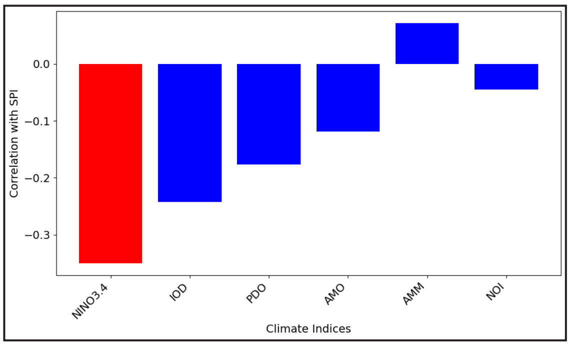

Figure 11. Correlation between SPI-12 and climate indices.

the analyses indicate that Niño 3.4, IOD, and PDO are closely interconnected. Among these indices, however, Niño 3.4 emerges as the most influential factor, demonstrating a dominant role in the observed relationships. Spatial mapping further illustrates this correlation framework, highlighting how these climate indices influence drought patterns across Java.

Each panel shows grid-point correlations between SPI-12 and a specific index: DMI (Indian Ocean Dipole), PDO, AMO, NOI, AMM, and Niño 3.4 (ENSO). Positive correlations are shown in blue to purple shades, while negative correlations are depicted in green to red (Figure 12).

Niño 3.4 and DMI exhibit strong negative correlations with SPI-12 across Central and East Java, indicating that El Niño and positive IOD phases were closely associated with reduced rainfall and intensified drought conditions during the 1960-1965 period. In contrast, PDO and AMO show predominantly positive correlations with SPI-12, especially in eastern and southern Java, suggesting that their positive phases may have moderate drought severity by contributing to increased rainfall. NOI and AMM display weaker and spatially inconsistent correlation patterns, reflecting a more limited or region-specific influence on drought variability during this timeframe.

Overall, the results highlight that ENSO-IOD interactions were the primary drivers of spatial

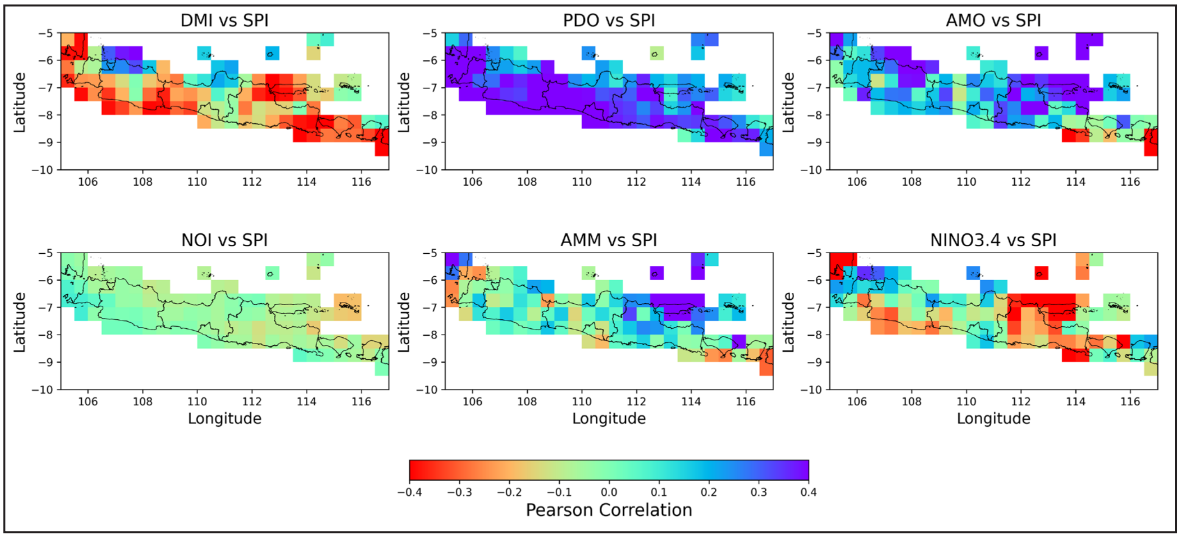

Figure 12. Spatial correlation between SPI-12 and climate indices (1960–1965).

drought variability in Java between 1960 and 1965, while decadal and Atlantic-related indices likely played a secondary or buffering role.

Discussion

In addition to prior studies on drought characteristics, research has increasingly focused on extreme drought conditions and their relation to large-scale climate indices in Indonesia. Previous studies have shown that drought duration, magnitude, and extent play critical roles in defining extreme drought events. Harisuseno (2020) found that droughts of longer duration in The Pekalen River Basin significantly reduced streamflow, highlighting that regions with prolonged droughts face critical water supply challenges.

Similarly, an analysis by Suhadi *et al.* (2023) in Sumatra, using SP and Effective Drought Index (EDI), revealed that areas undergoing extreme droughts often experienced SPI values below -2, a threshold indicative of serious water shortages. The spatial extent of drought is also critical; Wigati *et al.* (2025) mapped SPI-12 conditions across the Ciujung watershed and reported drought durations up to thirty-nine months in some stations, with SPI values reaching -3.46, underlining the compounding impact of wide spatial coverage and long persistence.

Large-scale climate indices further explain the variability of these drought events. The Niño 3.4 index, which measures temperature changes in the ocean's surface in the central equatorial Pacific, has a strong positive correlation with drought occurrences in Indonesia. For instance, (Phan-Van *et al*., 2022) demonstrated that El Niño phases (reflected in elevated Niño 3.4 values) were closely associated with suppressed rainfall and more frequent droughts in Southeast Asia, including Indonesia.

PDO also modulates Indonesian droughts. Lee (2015) found that PDO phases, in combination with ENSO, influence rainfall variability across Indonesia. Meanwhile, although the influence of AMO, AMM, and NOI is less directly documented in Indonesia, broader research indicates their teleconnection potential in shaping tropical rainfall patterns.

Integrating multiple climate indices, including Niño 3.4 and PDO into drought assessments enhances the predictive capability for extreme drought impacts. This integration is essential for water resource planning and agricultural resilience in a highly climate-sensitive country like Indonesia.

These findings have important implications for key sectors such as agriculture, water security, and environmental protection. Extreme droughts directly contribute to crop failures, groundwater depletion, and ecosystem degradation (Irawan and Komori, 2025). For example, long-term analyses in Indonesia have shown that agricultural droughts, especially when linked to large-scale climate variability, severely impact food production and rural livelihoods. Therefore, the results of this study are relevant for the development of climate-based early warning systems and drought mitigation policies. Studies have demonstrated that integrating indices like SPI and SPEI with ENSO-based forecasts enhances early warning capability in Southeast Asia (Phan-Van *et al.*, 2022). Furthermore, combining these climate indicators with watershed-based management strategies can strengthen adaptive responses at the regional level (Rohmat *et al*., 2023).

Although the analysis results show consistent patterns, this study has several limitations. One of the main challenges is the lack of complete observational rainfall data for the 1960s period, which prevents direct verification of the SPI-based findings. This is a common issue in long-term drought assessments in Indonesia, where historical climate records are often fragmented or unavailable prior to the 1980s (Irawan and Komori, 2025). In addition, limitations in the temporal and spatial resolution of the data, as well as the sensitivity of the SPI to long-term anomalies, may affect the accuracy of extreme drought event identification. For future research, it is recommended to use a combination of other drought indices, such as SPEI or PDSI, along with the integration of satellite data and climate reanalysis datasets to strengthen the robustness and validity of results (Phan-Van *et al.*, 2022).

Additionally, retrospective and prospective analysis of the 1960s Northeast U.S. drought shows that such severe events were linked to a combination of precipitation deficits and persistent high-pressure systems, and similar extreme droughts may become more frequent or severe due to climate change. This points out the urgent need for regional adaptation, resilient water resource strategies, and continuous climate monitoring to prevent widespread socio-economic and ecological losses (Xue and Ullrich, 2021).

In Java, extreme droughts occurred in 1960 and 1965, characterized by durations extending up to thirty-nine months. While not every drought year is extreme in duration, these specific events are recognized as such due to their longevity and severity. SPI-12 analysis reveals that drought conditions predominantly affected the southern half of Java Island, with nearly half the region impacted during these years. Moreover, a clear inverse correlation was observed between SPI-12 values and the Niño 3.4 index, reinforcing the influence of ENSO-driven temperature changes in the ocean on extreme drought occurrences in Java.

In drought studies, extreme drought is most commonly characterized based on its magnitude. However, an overreliance on magnitude alone may overlook another critical dimension of drought: its duration. Duration plays a crucial role, as prolonged drought periods, even with relatively moderate magnitudes, can lead to significant impacts. In addition, duration should also be considered in the context of extreme conditions, where extended periods of very low SPI values (*e.g.* SPI ≤ -2) may indicate particularly severe and persistent drought events. A more detailed exploration of duration-based drought classification will be addressed in subsequent work.

Conclusions

The analysis of extreme drought characteristics over Java Island from 1960 to 1965 yields several important insights. Severe drought episodes occurred notably in 1960 and 1965, while 1964 stood out for its extreme magnitude, indicated by SPI values equal to or below -2. These droughts were particularly prolonged, lasting up to thirty-nine months. Spatial analysis of SPI-12 further reveals that drought conditions were concentrated in the southern half of Java Island, with nearly half the region affected during the study period.

Moreover, spatial correlation analysis highlights the dominant influence of large-scale climate drivers, particularly ENSO and the Indian Ocean Dipole, on drought variability in Java. The

Niño 3.4 and DMI indices showed the strongest negative correlations with SPI-12, especially across Central and East Java, confirming their role in amplifying rainfall deficits. In contrast, the PDO exhibited a predominantly positive correlation with SPI-12, suggesting that positive PDO phases may have moderate drought severity by enhancing rainfall. These findings emphasise the necessity of accounting for both interannual and decadal climate variability in drought prediction and water resource planning across the region.

Acknowledgement

This research was supported by the Faculty of Earth Sciences and Technology (FITB) at Institut Teknologi Bandung through the PPMI FITB 2026 scheme (Contract Number 2235/IT1.B07.1/TA.00/2026). The authors are grateful for the constructive feedback received from the reviewers, which greatly improved this work.

References

Avia, L.Q., Yulihastin, E., Izzaturrahim, M.H., Muharsyah, R., Satyawardhana, H., Sofiati, I., Nurfindarti, E., and Gammamerdianti, 2023. The spatial distribution of a comprehensive drought risk index in Java, Indonesia. *Kuwait Journal of Science*, 50 (4), p.753-760. https://doi.org/10.1016/j.kjs.2023.02.031.

Cunha, A.P.M.A., Zeri, M., Deusdará Leal, K., Costa, L., Cuartas, L.A., Marengo, J.A., Tomasella, J., Vieira, R.M., Barbosa, A.A., Cunningham, C., Cal Garcia, J.V., Broedel, E., Alvalá, R., and Ribeiro-Neto, G., 2019. Extreme Drought Events over Brazil from 2011 to 2019. *Atmosphere*, 10 (11), 642. https://doi.org/10.3390/atmos10110642.

Dai, A., 2011. Drought under global warming: A review. *WIREs Climate Change*, 2 (1), p.45-65. https://doi.org/10.1002/wcc.81.

D’Arrigo, R., Wilson, R., Palmer, J., Krusic, P., Curtis, A., Sakulich, J., Bijaksana, S., Zulaikah, S., and Ngkoimani, L.O., 2006. Monsoon drought over Java, Indonesia, during the past two centuries. *Geophysical Research Letters*, 33 (4), p.1-4. https://doi.org/10.1029/2005GL025465.

Guo, Y., Huang, S., Huang, Q., Leng, G., Fang, W., Wang, L., and Wang, H., 2020. Propagation thresholds of meteorological drought for triggering hydrological drought at various levels. *Science of The Total Environment*, 712, 136502. https://doi.org/10.1016/j.scitotenv.2,020.136502.

Harisuseno, D., 2020. Meteorological Drought and its Relationship with Southern Oscillation Index (SOI). *Civil Engineering Journal*, 6 (10), p.1864-1875. https://doi.org/10.28991/cej-2020-03091588.

Irawan, A.N.R. and Komori, D., 2025. Long-term variability of agricultural drought’s characteristic in Indonesia. *Journal of Agricultural Meteorology*, 81 (4), p.203-213. https://doi.org/10.2480/agrmet.D-24-00024.

Lee, H.S., 2015. General Rainfall Patterns in Indonesia and the Potential Impacts of Local Seas on Rainfall Intensity. *Water*, 7 (4), p.1751-1768. https://doi.org/10.3390/w7041751.

Loon, A.F. van, Tijdeman, E., Wanders, N., Lanen, H.a.J. van, Teuling, A.J., and Uijlenhoet, R., 2014. How climate seasonality modifies drought duration and deficit. *Journal of Geophysical Research: Atmospheres*, 119 (8), p.4640-4656. https://doi.org/10.1002/2013JD020383.

McKee, T.B., Doesken, N.J., and Kleist, J., 1993. *The Relationship of Drought Frequency and Duration to Time Scales*. Eighth Conference on Applied Climatology.

Mishra, A.K. and Singh, V.P., 2010. A review of drought concepts. *Journal of Hydrology*, 391 (1-2), p.202-216. https://doi.org/10.1016/j.jhydrol.2010.07.012.

Mulsandi, A., Koesmaryono, Y., Hidayat, R., Faqih, A., and Sopaheluwakan, A., 2023. On The Interannual Variability of Indonesian Monsoon Rainfall (IMR): A Literature Review of The Role of its External Forcing. *Jurnal Meteorologi dan Geofisika*, 24 (2), p.115-127. https://doi.org/10.31172/jmg.v24i2.1049.

Phan-Van, T., Nguyen-Ngoc-Bich, P., Ngo-Duc, T., Vu-Minh, T., Le, P.V.V., Trinh-Tuan, L., Nguyen-Thi, T., Pham-Thanh, H., and Tran-Quang, D., 2022. *Drought over Southeast Asia and Its Association with Large-Scale Drivers*. https://doi.org/10.1175/JCLI-D-21-0770.1.

Riebsame, W.E., Changnon, S.A., and Karl, T.R., 2019. *Drought and Natural Resources Management in the United States: Impacts and Implications of the 1987−89 Drought* (1st ed.). Routledge. https://doi.org/10.4324/9780429045332.

Rohmat, F.I.W., Harjupa, W., Rohmat, D., and Rohmat, F.I.W., 2023. The impacts of global atmospheric circulations on the water supply in select watersheds in the Indonesian Maritime Continent using SPI. *Heliyon*, 9 (5), p.1-15. e15604. https://doi.org/10.1016/j.heliyon.2023.e15604.

Ropelewski, C.F. and Halpert, M.S., 1987. *Global and Regional Scale Precipitation Patterns Associated with the El Niño/Southern Oscillation*. https://journals.ametsoc.org/view/ journals/mwre/115/8/1520-0493_1987_115_1606_garspp_2_0_co_2.xml.

Saji, N.H., Goswami, B.N., Vinayachandran, P.N., and Yamagata, T., 1999. A dipole mode in the tropical Indian Ocean. *Nature*, 401(6751), p.360-363. https://doi.org/10.1038/ 43854.

Smith, S.J., Edmonds, J., Hartin, C.A., Mundra, A., and Calvin, K., 2015. Near-term acceleration in the rate of temperature change. *Nature Climate Change*, 5 (4), p.333-336. https://doi.org/10.1038/nclimate2552.

Spinoni, J., Naumann, G., and Vogt, J.V., 2017. Pan-European seasonal trends and recent changes of drought frequency and severity. *Global and Planetary Change*, 148, p.113-130. https://doi.org/10.1016/j.gloplacha.2016.11.013.

Suhadi, S., Iskandar, I., Supari, S., Irfan, M., and Akhsan, H., 2023. Extreme Drought Assessment in Sumatra-Indonesia Using SPI and EDI. *Science and Technology Indonesia*, 8 (4), p.691-700. https://doi.org/10.26554/sti.2023.8.4.691-700.

Suwarman, R., Ichiyanagi, K., Tanoue, M., Yoshimura, K., Mori, S., Yamanaka, M.D., Syamsudin, F., and Belgaman, H.A., 2017. El Niño Southern Oscillation Signature in Atmospheric Water Isotopes over Maritime Continent during Wet Season. *Journal of the Meteorological Society of Japan. Ser. II*, 95 (1), p.49-66. https://doi.org/10.2151/jmsj.2017-003.

Tallaksen, L.M. and Lanen, H. van, 2004. *Hydrological Drought: Processes and Estimation Methods for Streamflow and Groundwater*.

Tangang, F.T., Juneng, L., and Ahmad, S., 2007. Trend and interannual variability of temperature in Malaysia: 1961-2002. *Theoretical and Applied Climatology*, 89 (3-4), p.127-141. https://doi.org/10.1007/s00704-006-0263-3.

Ul Hassan, W. and Ahmad Nayak, M., 2021. Global teleconnections in droughts caused by oceanic and atmospheric circulation patterns. *Environmental Research Letters*, 16. https://doi.org/10.1088/1748-9326/abc9e2.

Wang, S., Huang, J., He, Y., and Guan, Y., 2014. Combined effects of the Pacific Decadal Oscillation and El Niño-Southern Oscillation on Global Land Dry–Wet Changes. *Scientific Reports*, 4 (1), 6651. https://doi.org/10.1038/srep06651.

Wigati, R., Fathonah, W., Putu Purnaditya, N., Mina, E., and Susilawati, 2025. Drought Mapping Using Standardized Precipitation Index (SPI) Ciujung Watershed, Indonesia. *Applied Research on Civil Engineering and Environment (ARCEE)*, 6 (01), p.51-62. https://doi.org/10.32722/arcee.v6i01.6961.

WMO, 2012. *Standardized Precipitation Index User Guide*. World Meteorological Organization.

WMO, 2023. *Guidelines on the Definition and Characterization of Extreme Weather and Climate Events*. World Meteorological Organization.

Xue, Z. and Ullrich, P., 2021. A Retrospective and Prospective Examination of the 1960s U.S. Northeast Drought. *Earth's Future*, 9 (7), p.1-27. e2020EF001930. https://doi.org/10.1029/2020EF001930.